APL Materials

RESEARCH ARTICLE | AUGUST 04 2023

Overcoming the compensation of acceptors in GaN:Mg by defect complex formation

Special Collection: Challenges and Perspectives in Materials Chemistry—A Celebration of Prof. Sir Anthony K. Cheetham's 75th Birthday

Zijuan Xie; John Buckeridge; C. Richard A. Catlow; Anping Zhang; Thomas W. Keal; Paul Sherwood; You Lu; Scott M. Woodley; Alexey A. Sokol

APL Mater 11, 080701 (2023)
https://doi.org/10.1063/5.0148858

APL Materials RESEARCH UPDATE pubs.aip.org/aip/apm

Overcoming the compensation of acceptors in GaN:Mg by defect complex formation

Cite as: APL Mater. 11, 080701 (2023); doi: 10.1063/5.0148858
Submitted: 2 March 2023 • Accepted: 12 July 2023 •
Published Online: 4 August 2023

Zijuan Xie,[1,2,a)] John Buckeridge,[3,a)] C. Richard A. Catlow,[2,4] Anping Zhang,[1] Thomas W. Keal,[5] Paul Sherwood,[5] You Lu,[5] Scott M. Woodley,[2] and Alexey A. Sokol[2,a)]

AFFILIATIONS

[1] International School of Microelectronics, Dongguan University of Technology, 523808 Dongguan, People's Republic of China
[2] Department of Chemistry, Kathleen Lonsdale Materials Chemistry, University College London, WC1 HOAJ London, United Kingdom
[3] School of Engineering, London South Bank University, SE1 0AA London, United Kingdom
[4] School of Chemistry, Cardiff University, Park Place, CF10 1AT Cardiff, United Kingdom
[5] Scientific Computing Department, STFC Daresbury Laboratory, Daresbury, Warrington WA4 4AD, United Kingdom

Note: This paper is part of the Special Topic on Challenges and Perspectives in Materials Chemistry—A Celebration of Professor Sir Anthony K. Cheetham's 75th Birthday.

[a)] **Authors to whom correspondence should be addressed:** zjxie@dgut.edu.cn; j.buckeridge@lsbu.ac.uk; and a.sokol@ucl.ac.uk

ABSTRACT

In GaN:Mg, the Mg_{Ga} acceptor is compensated extensively by the formation of nitrogen vacancies (V_N) and Mg interstitials (Mg_i). However, we show that such compensation can be overcome by forming two kinds of Mg-rich complexes: one that contains V_N and the other that contains only Mg_{Ga} and Mg_i. Such complexing not only neutralizes V_N and Mg_i but also forms better complex acceptors that have lower formation energies and smaller hole localization energies than isolated Mg_{Ga}. Our results help explain the different doping behaviors in samples grown by different methods.

I. INTRODUCTION

The realization of *p*-type conductivity in GaN:Mg has enabled the application of GaN-based electronic and optical devices. However, such industrial success is achieved under the shadow of a poor understanding of the underlying mechanism, despite decades of academic research. The *p*-type conductivity of GaN can be achieved only by heavily doping with Mg, with concentrations of Mg above 10^{19} cm^{-3} in metalorganic chemical vapor deposition (MOCVD) grown samples,[1] for example. According to Hall-effect measurements of MOCVD GaN:Mg layers by Kaufmann *et al.*[2] the hole concentration reaches a maximum value of 6×10^{17} cm^{-3} at an Mg concentration of 2×10^{19} cm^{-3}, then decreases at higher Mg concentrations. The photoluminescence (PL) bands in undoped and Mg-doped GaN can help clarify the electronic properties, yet their attribution is still under debate. The ultraviolet luminescence (UVL) band is the dominant PL band in conductive *n*-type undoped and Mg-doped GaN grown by different techniques, as well as in conductive *p*-type Mg-doped GaN grown by molecular beam epitaxy (MBE). The blue luminescence (BL) band is observed only in GaN:Mg samples grown by hydride vapor phase epitaxy (HVPE) or MOCVD when the concentration of Mg exceeds 10^{19} cm^{-3}.[1] Kaufmann *et al.*[3] connected the emergence of the room temperature (RT) PL band that peaks around 2.8 eV with the maximum value of the hole density reached as a function of Mg concentration for Mg concentration of $(1–2) \times 10^{19}$ cm^{-3} in MOCVD-grown GaN and presented clear evidence for the distant donor–acceptor (D–A) pair character of the 2.8 eV band. The reasons for the absence of *p*-type conductivity under moderate Mg doping, the onset of *p*-type conductivity under heavy Mg doping, and the subsequent drop-off in conductivity after reaching a maximum value of the hole concentration, as well as the origin of the UVL and BL in GaN:Mg, have

been debated intensively for a few decades now, without resolution so far.

To date, the attribution of the electronic and optical properties of GaN:Mg to particular defect states remains unclear. Several models have been proposed. Apart from the commonly calculated deep levels of acceptors in wide bandgap semiconductors that localize a hole at single anion ligand atoms with a Jahn-Teller type symmetry breaking, Lany and Zunger[4] found an effective-mass-like delocalized state of Mg_{Ga} acceptors in GaN, which, in contrast, has a symmetric configuration. Despite the large geometry distortion in the localized state, this dual nature has a small energy difference of 0.03 eV, according to their calculation employing a Koopmans-corrected density functional theory (DFT) method. They predicted that the shallow state would dominate in *n*-type samples, whereas in less compensated *p*-type samples, the deep state would dominate. Lyons *et al.*,[5] with hybrid DFT calculations, computed a relatively shallow (0/−) thermodynamic transition level for Mg_{Ga} (260 meV), which they found to exhibit key features of a deep acceptor: the hole is localized on an N atom neighboring the Mg impurity, inducing a large local lattice distortion and giving rise to broad blue luminescence. Therefore, they attributed the BL to Mg_{Ga} and the UVL to Mg_{Ga}-H_i. They found no evidence for the existence of other metastable configurations, in contrast to Lany and Zunger. Using hybrid DFT calculations, however, Sun *et al.*[6] found Mg_{Ga} in GaN has a configuration characterized by highly anisotropic polaron localization that exhibits both effective-mass-like and noneffective-mass-like characters, similar to the result of Lany and Zunger. Their calculations were reproduced by Demchenko *et al.*,[7] who attributed the UVL band to the anisotropically delocalized acceptor state. In earlier work, using the hybrid quantum mechanical (QM) and molecular mechanical (MM) embedded cluster method,[8] we found that in lightly doped GaN:Mg, isolated Mg_{Ga} strongly trap holes and, therefore, do not contribute to *p*-type conduction.

Whether the model involving only isolated Mg_{Ga} defects, which may have a dual nature, is sufficient to account for the observed *p*-type conductivity and different PL bands or whether more complicated defects (complexes) have to be included has also drawn controversy in experimental studies. Monemar *et al.*[9] studied bound-exciton spectra in samples for Mg concentrations up to $[Mg] \approx 10^{19}$ cm^{-3} and found evidence for two Mg-related acceptors in GaN. The unstable UVL emission peaking at 3.27 eV upon *p*-type activation was thus attributed to one of the two acceptors, which is unstable in *p*-GaN. Later, Monemar *et al.*[10] attributed these two acceptors to isolated Mg_{Ga} and a deeper acceptor that arises due to the interaction between basal plane stacking faults and Mg_{Ga} acceptors. The dual nature model of Lany and Zunger was supported by Callsen *et al.*[11] from the optical signature of Mg-doped GaN through the determination of the binding energies of two Mg acceptor states, while their sample was lightly Mg-doped (8×10^{17} cm^{-3}). Singh *et al.*[12] probed the lattice location of Mg in doubly doped GaN (Mg):Eu and linked two distinct Eu–Mg defect configurations with Lany and Zunger's model. Electron paramagnetic spin resonance (EPR) and optically detected magnetic resonance (ODMR) measurements, along with PL, have also been performed to investigate acceptors in GaN:Mg. Glaser *et al.*[13] performed ODMR and found a highly anisotropic g-tensor associated with the 3.27 eV PL emission from lightly Mg-doped samples predicted for effective-mass Mg acceptors in GaN. Later, (basal-plane) strain was highlighted as playing a crucial role in influencing the detailed nature of the acceptor states: the shallow effective-mass-like acceptor and deeper acceptor states are attributed to simple substitutional Mg at Ga sites in unstrained and strained regions, respectively.[14,15]

It is clear from the above-mentioned discussion that there is no single model that can satisfactorily explain the evolution of the *p*-type conductivity or the observed PL signals upon Mg doping. The electrical activation of Mg as a *p*-type dopant requires its incorporation into substitutional Ga as a single acceptor, while donor type defects such as N vacancies, Mg interstitials, or impurities such as hydrogen and silicon are likely to compensate, making Mg_{Ga} a "vulnerable" acceptor dopant (giving rise to the observed doping limit[16]).

The nitrogen vacancy V_N, as an intrinsic defect, has long been proposed as a major compensating center in GaN:Mg. By using room temperature Hall-effect measurements as a function of the Mg concentration, Kaufmann *et al.*[2] found evidence for self-compensation, i.e., dopant-driven compensation of the Mg acceptor after reaching the maximum hole concentration by intrinsic donor defects rather than donor impurities, for which they developed a self-compensation model involving nitrogen vacancies. For heavily doped materials, they favored the V_N-Mg_{Ga} pair model. Applying positron annihilation spectroscopy, Hautakangas *et al.*[17] recorded a positron lifetime of 180 ps in MOCVD grown Mg-doped GaN and suggested that neutral or negative complexes involving the mono-vacancy V_N, in particular the V_N-Mg_{Ga} complex, were present in semi-insulating and *p*-type GaN. Interestingly, they observed no vacancies in MBE grown GaN:Mg layers. By performing Hall-effect, secondary-ion-mass spectroscopy (SIMS), and Rutherford backscattering spectrometry (RBS)-channeling measurements, Obata *et al.*[18] investigated the lattice properties of heavily Mg-doped GaN and found that the lattice relaxation of nitrogen atoms is much higher than for Ga atoms, suggesting that the inverted *n*-type conductivity is caused by self-compensation effects induced by nitrogen vacancies. Using DFT calculations, Myers *et al.*[19] indicated that V_N compensates Mg acceptors extensively at higher doping levels. By employing a hybrid functional, Yan *et al.*[20] found that both Mg_{Ga}-V_N and V_N act as compensating centers in *p*-type GaN. Lee *et al.*[21] studied three Mg-H-V_N complexes in GaN:Mg and found that the inclusion of V_N in many of the passivated complexes is necessary, given their abundance and energetic favorability in GaN:Mg. Using the QM/MM embedded cluster method,[8] we previously determined that the nitrogen vacancy is a shallow compensating center in GaN doped with divalent metals, and consequently, isolated Mg_{Ga} alone cannot account for the *p*-type conductivity in GaN:Mg. We calculated the optical level associated with V_N at 44 meV below the conduction band minimum (CBM), to which we attributed the observed 3.466 eV UVL peak.

Apart from the nitrogen vacancy, there is evidence that the Mg interstitial (Mg_i) is also a major compensating center in GaN:Mg. Early electronic structure calculations by Reboredo and Pantelides[22] showed that Mg_i and its complexes play a significant role in controlling the *p*-type doping process; they found that compensation of Mg_{Ga}^{-} occurs mainly through the formation of Mg substitutional-interstitial pairs, among others, while H impurities can passivate them all. More recently, low formation energies for Mg_i when the Fermi level is located below midgap have been computed.[23] Miceli and Pasquarello,[24] using hybrid DFT, found that the Mg_i

shows a noticeably lower free energy of formation than the Mg_{Ga} in *p*-type conditions and, together with nitrogen vacancies, will act as a compensating center for donors. Recently, by implanting radioactive ^{27}Mg into GaN, Wahl *et al.*[25] gave direct experimental evidence for Mg_i near octahedral sites and showed a significant concentration of Mg_i in *p*-type GaN. Later, Wahl *et al.* elucidated the amphoteric nature of Mg, i.e., the concurrent occupation of substitutional Ga and interstitial sites. They concluded that challenges toward high electrical activation of implanted Mg are not related to a lack of substitutional incorporation.[26] Along with other divalent metals, Be, for example, has also been investigated as an alternative *p*-type dopant; however, self-compensation induced by interstitials is likely to be considerably more pronounced for Be than for Mg, which would explain why no successful synthesis of *p*-type GaN:Be has been reported as yet.[27]

To achieve *p*-type conductivity, the compensation effects of V_N and Mg_i induced inevitably by heavy Mg doping must be controlled. In this paper, we study complexes comprising the acceptor Mg_{Ga} and the donors V_N and Mg_i. We show that V_N as a triple donor in *p*-GaN must be passivated; Mg_{Ga} as the only acceptor-type defect has to contribute to *p*-type conductivity, possibly by forming acceptor complexes; and Mg_i as a double donor needs to be passivated in *p*-type GaN and can account for the doping threshold. We find that a large complex with Mg_3N_2 stoichiometry passivates V_N and Mg_i, and with one more Mg_{Ga} as an acceptor— improves the *p*-type behavior of the dopant, a trend we postulate may continue for even larger clusters, although the small clusters studied here cannot explain *p*-type doping by themselves. We conclude that there could be two different acceptors: Mg-rich complexes with and without an N vacancy, which can explain the different doping behavior in GaN:Mg samples— grown by different methods.

II. COMPUTATIONAL DETAILS

In this work, electronic properties of defects and their complexes in wurtzite GaN:Mg are obtained following a hybrid QM/MM embedded cluster approach, which has been developed to describe localized states in ionic solids where charged and strong polar centers interact via long-range Coulomb and short-range Pauli repulsion forces.[28,29] This method splits extended systems into the inner region, containing the centrally located defect, described using molecular QM theories, and its surroundings, which are only lightly perturbed by the defect, modeled with MM techniques based on interatomic potentials. Our choice of the QM methodology is DFT; the MM simulations employ polarizable-shell model interatomic potentials. The interface between the inner and outer regions employs cation-centered semi-local pseudopotentials to provide an appropriate embedding potential acting on the electronic subsystem of the defect and to contain the electrons within the inner region, effectively preventing them from spilling over the positively charged, attracting cations residing in the outer MM region. The outer part of the MM region is held fixed at the pre-optimized geometry,[8,28] and any polarization here is treated *a posteriori*. The entire cluster is surrounded by point charges, whose values are fitted to reproduce the Madelung potential of the infinite crystal within the inner QM region along with its immediate MM environment, all contained within an "active sphere" of a user-defined radius (typically 15–20 Å). Using the embedded cluster approach with a suitably terminated QM cluster (i.e., with cations as terminating ions and an appropriate embedding potential), we can model the well localized valence band maximum (VBM) states. Therefore, by calculating the ionization energy of an electron in the bulk system, we can probe the VBM and determine its position relative to the vacuum. We then shift the CBM at an energy equal to the bandgap (3.5 eV) above the VBM relative to the vacuum. The advantage of our approach is the comprehensive account of short- and long-range polarization effects due to the presence of charged defects, the lack of periodic image interactions, the true infinitely dilute limit when reporting defect energetics, and an unambiguous definition of the vacuum level, facilitating the calculation of ionization energies with an absolute reference.

The method has been implemented in the ChemShell package,[28,29,31] employing GAMESS-UK[32] for the QM single-point energy and gradient calculations and GULP[33] for the MM calculations. The QM region of 6.8 Å radius (116 atoms of wurtzite GaN) is embedded in an MM region of radius 30 Å. In our QM calculations, we use (i) the hybrid exchange and correlation density functional B97-2,[34] which is similar to those commonly used in plane-wave supercell calculations (21% exact exchange compared with 25% for PBE0[35] or HSE06[36]), (ii) the SBKJC small-core pseudopotentials on Ga[37] within the cluster and large-core refitted pseudopotentials[8,30] on the cations forming the interface, and (iii) the atom-centered Gaussian basis set of def2-TZVP form on N[38] and a matching quality SBKJC basis on Ga.[37] For comparison, we use a second hybrid exchange and correlation density functional, BB1K, employing 42% exact exchange[39] and fitted to reproduce kinetic barriers and thermochemical data, which removes a significant portion of the self-interaction error in exchange and correlation, thus giving a more accurate description of electron and hole localization and consequently deeper transition levels with respect to the VBM.[40] Other computational details can be found in our earlier publication.[28,41] We have applied this method previously to treat defects in AgCl,[42] ZnO,[43,44] and in earlier studies of GaN.[8,40,45,46]

III. RESULTS AND DISCUSSION

We first show the formation energies under anion-rich conditions of the three important defects in *p*-GaN:Mg, as discussed earlier: V_N, Mg_{Ga}, and Mg_i, in Figs. 1(a) and 1(b). We note that V_N has been discussed in detail in our previous work.[8,40] The formation energies of Mg_{Ga} are reproduced from Ref. 8, but here we include a +/0 transition at 0.37 (0.84) eV above the VBM, determined using the B97-2 (BB1K) functional. Mg_i stabilizes at an octahedral interstitial site in the hexagonal channel of wurtzite GaN, similar to Ga_i.[40] Mg_i is a donor-like defect for Fermi level values across the bandgap, stabilizing in the +2 charge state, and the formation energy at the VBM is −0.59 (−2.68) eV, computed using the B97-2 (BB1K) functional. For Fermi levels in the lower part of the bandgap, the formation energies of V_N and Mg_i are negative and lower than those of Mg_{Ga}, implying spontaneous formation and a compensating nature for both. The low formation energies of V_N and Mg_i in *p*-GaN have also been reported in studies employing supercell calculations.[20,23,24] Reshchikov *et al.* performed hybrid DFT calculations [using a modified Heyd–Scuseria–Ernzerhof (HSE) functional[36] with an exact exchange fraction of 0.312] and found low formation energies of V_N and Mg_i near the VBM and the 0/− transition level of Mg_{Ga}

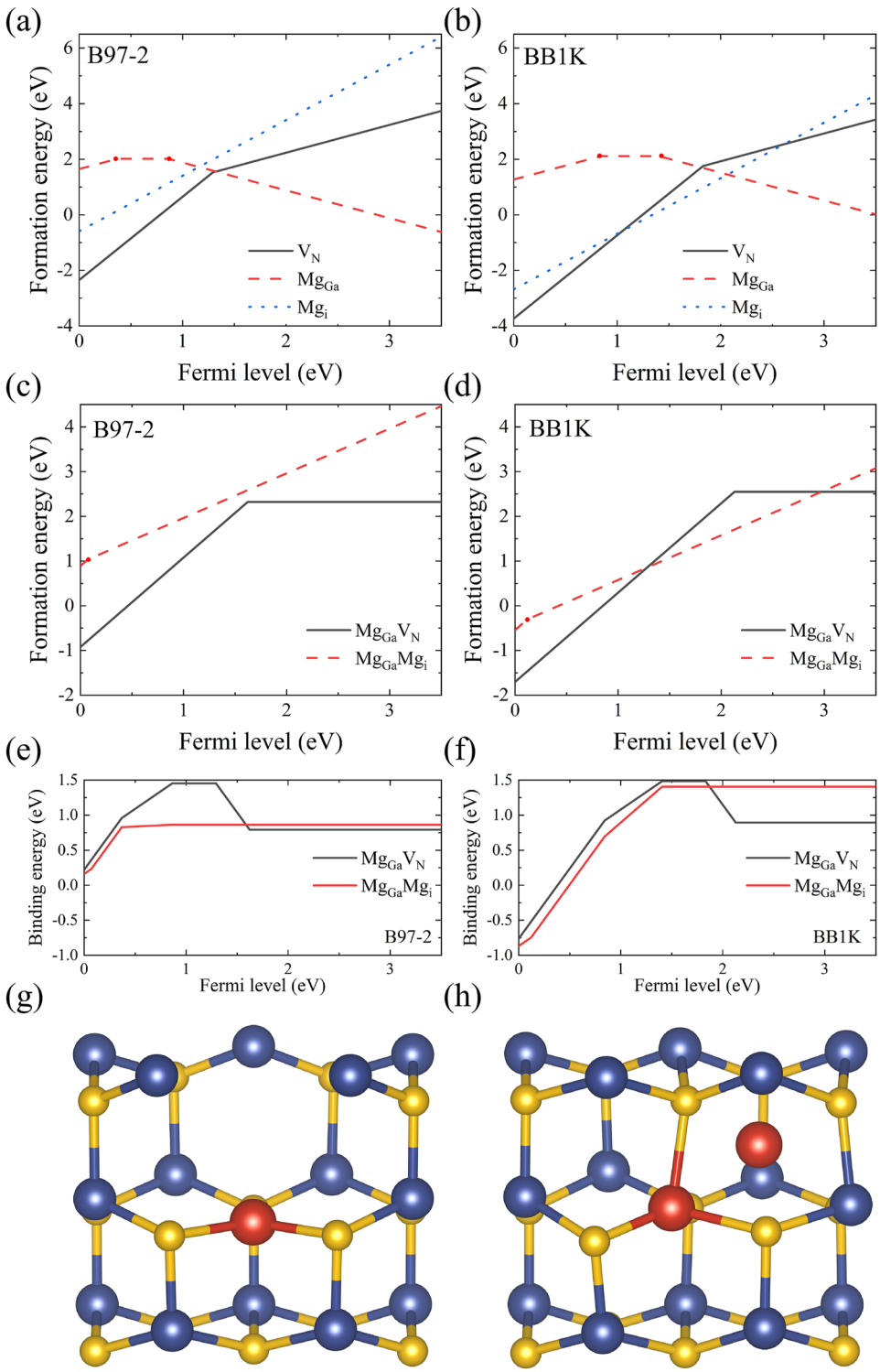

FIG. 1. (a) B97-2 and (b) BB1K calculated—formation energies of V_N (black line), Mg_{Ga} (red line), and Mg_i (blue line) as a function of Fermi energy above the VBM. (c) and (e) B97-2 and (d) and (f) BB1K calculated—formation energies and binding energies of the complexes Mg_{Ga}-V_N (black line) and Mg_{Ga}-Mg_i (red line). Positive binding energies indicate favorable binding. Anion-rich conditions are assumed in (a)–(f). Structures of (g) Mg_{Ga}-V_N in a +2 charge state and (h) Mg_{Ga}-Mg_i in a +1 charge state. The blue, yellow, and red balls denote the Ga, N, and Mg atoms, respectively.

at 0.326 eV above the VBM.[23] Miceli and Pasquarello performed similar hybrid DFT calculations (HSE functional with 0.31 exact exchange) and found similar low formation energies of V_N and Mg_i near the VBM and the 0/− transition level of Mg_{Ga} at 0.38 eV above the VBM.[24] Our results are consistent with the trend of the Mg_{Ga} thermodynamic transition levels moving deeper into the gap with charged defects treated by our method compared with supercell calculations and with an increasing exact exchange fraction included in hybrid functionals, as detailed in Ref. 40. We thus confirm the compensating effects of V_N and Mg_i, a result largely independent of the functional or model used.[47,48] Similar compensating effects have been found in GaN:Be.[49]

As triple- and double-donor defects in *p*-GaN, respectively, we expect V_N and Mg_i to easily bind the acceptor Mg_{Ga} and form complexes Mg_{Ga}-V_N and Mg_{Ga}-Mg_i. We calculate three configurations of Mg_{Ga}-V_N, where the missing N, relative to the Mg_{Ga}, is on either an axial site, a basal-plane site, or a next-nearest neighbor site. We find that these configurations all have very similar formation energies, and we present the results only for the axial site configurations.[59] Mg_{Ga}-Mg_i is composed of Mg_i with a neighboring Ga replaced by Mg. Figures 1(c) and 1(d) show the formation energies of these two complexes under anion-rich conditions (under anion-poor conditions, the formation energies will be 1.59 and 2.04 eV lower, respectively). They are donor-like in the *p*-type region (i.e., Fermi level values in the lower half of the gap) and have negative formation energies close to the VBM, so they will act as compensating centers. Comparing Figs. 1(a)–1(d), we see that binding a Mg_{Ga} results in V_N and Mg_i centers with slightly higher formation energies but, crucially, lower positive charge states in the *p*-type region and, consequently, less severe compensating centers as complexes than as isolated species. Note that the positive binding energies in Figs. 1(e) and 1(f) of these two complexes imply that they are bound species.[45] Structures of Mg_{Ga}-V_N in the +2 charge state and Mg_{Ga}-Mg_i in the +1 charge state are shown in Figs. 1(g) and 1(h), respectively. The substitutional Mg_{Ga}, as an isolated defect, tends to have associated with it a localized hole on a nearest-neighbor N ion in its neutral charge state and a second localized hole on another nearest neighbor N ion when the Fermi level is very close to the VBM (the defect is then in the + state). The energy needed to dissociate the localized hole is quite large, 1.404 eV as computed with the BB1K functional; therefore, the activation of Mg_{Ga}^{-} and subsequent *p*-type conductivity are difficult to achieve. However, through binding a donor defect, the hole localized by Mg_{Ga} recombines with a donor electron. Note that in both complexes, Mg_{Ga} is in its state of −1 throughout the bandgap, except in Mg_{Ga}-Mg_i when the Fermi level is less than 0.07 (0.012) eV above the VBM for the B97-2 (BB1K) functional. Therefore, in *p*-GaN, these complexes will act as donors, but the Mg_{Ga}-Mg_i complex can release a trapped hole with an energy of 0.07 or 0.012 eV. However, crucially, both complexes can serve as nucleation centers for larger complexes, which may act as acceptors, as we show below.

The Mg_{Ga}-V_N complex has been studied several times previously. However, the Mg_{Ga}-Mg_i complex is much less well studied[22] since the role of Mg_i has only recently been appreciated. We compare our calculated formation energies of both complexes in the neutral charge state only with those determined using supercells since the periodic image interactions are particularly problematic for charged defects. For neutral Mg_{Ga}-V_N, we determine a formation energy of 2.32 (2.55) eV in N-rich conditions and 0.73 (0.96 eV) in N-poor conditions using the B97-2 (BB1K) functional, compared with supercell-method-calculated values of 2.8 eV (N-rich) and 2 eV (N-poor),[20] 2.1 eV (N-rich) and 1.25 (N-poor),[24] determined with HSE, and 0.13 eV (N-poor),[19] and 1.6 eV (N-poor)[50] determined in earlier DFT studies. The compensating effects of Mg_{Ga} and Mg_{Ga}-V_N have been investigated using various measurement techniques.[2,17,18] Although V_N are very difficult to detect experimentally due to either the small size of the vacancy, the high concentrations of other defects, or the requirements for negative and neutral charge states, depending on the experimental method,[51] Hautakangas *et al.*[17] proposed Mg_{Ga}-V_N complexes as native defects in Mg-doped GaN using positron annihilation spectroscopy (PAS). They attributed their measured 180 ps positron lifetime to V_N or related complexes. As the isolated V_N will not act as a positron trap because of its positive charge, they suggested that neutral or negative complexes involving V_N are present in GaN:Mg. From computed core-electron momentum distributions, they identified Mg_{Ga}-V_N as the source of the observed positron lifetime. Mg_{Ga}-V_N is not neutral or negative in *p*-type GaN, as can be seen from our calculations and those of others referenced earlier. Mg_{Ga}-V_N is in the charge state of +2 until the +2/0 transition at 1.62 (2.13) eV above the VBM in Fig. 1(c) [and Fig. 1(d)]. Hybrid functional supercell calculations show this transition at ∼ 0.8 eV[20,24,50] above the VBM. Like isolated V_N, Mg_{Ga}-V_N has a positive charge state in *p*-type GaN and is unlikely to be a positron trap.

Mg_{Ga}-V_N and Mg_{Ga}-Mg_i, although less severe, are still compensating centers in *p*-type GaN, just like isolated V_N and Mg_i, respectively. Therefore, as double and single donor defects in *p*-GaN, we expect them to continue binding Mg_{Ga} and to form complexes. Moreover, we expect such larger complexes to further reduce the compensating effect of such centers and help free holes from localization to Mg_{Ga}, which may finally result in *p*-type conductivity in GaN:Mg.

Therefore, we calculate two Mg-rich complexes, $4Mg_{Ga}$-V_N and $3Mg_{Ga}$-Mg_i, where V_N and Mg_i are fully neutralized, and these two complexes are acceptors as a whole. $4Mg_{Ga}$-V_N is composed of a N vacancy with its four nearest Ga all replaced by Mg, as shown in Fig. 2(a). In its closed-shell configuration of charge state −, the axial Mg_{Ga} moves away from the vacant site by 43% (44%) of the equilibrium Ga–N bond length, while the other three basal Mg_{Ga} move away by 19% (17%), as calculated using the B97-2 (BB1K) functional. When its charge state changes from − to 0 and then to +, Mg_{Ga} moves farther away from the vacancy site by 4% when a hole is localized on a bonded N atom of Mg_{Ga}. $3Mg_{Ga}$-Mg_i is composed of an octahedral site Mg_i with three of its six nearest Ga replaced by Mg, so we calculate one of six possible configurations, shown in Fig. 2(d). In Figs. 2(b), 2(c), 2(e), and 2(f), we show the formation energies in both conditions for these two complexes. They both have a lower formation energy under anion-poor conditions since the isolated Mg_{Ga}, V_N, and Mg_i all favor anion-poor conditions. Comparing these two acceptor complexes with the isolated Mg_{Ga} in Figs. 1(a) and 1(b), we find using the B97-2 functional (BB1K functional) that the 0/− transition level has been reduced from the isolated Mg_{Ga} value of 0.863 (1.404) eV to 0.655 (0.997) and 0.690 (1.178) eV above the VBM, respectively, indicating that less energy is needed to dissociate a hole than that localized by isolated Mg_{Ga}. Note that the Mg_{Ga}-Mg_i complex has a negative *U* effect, with a +/−

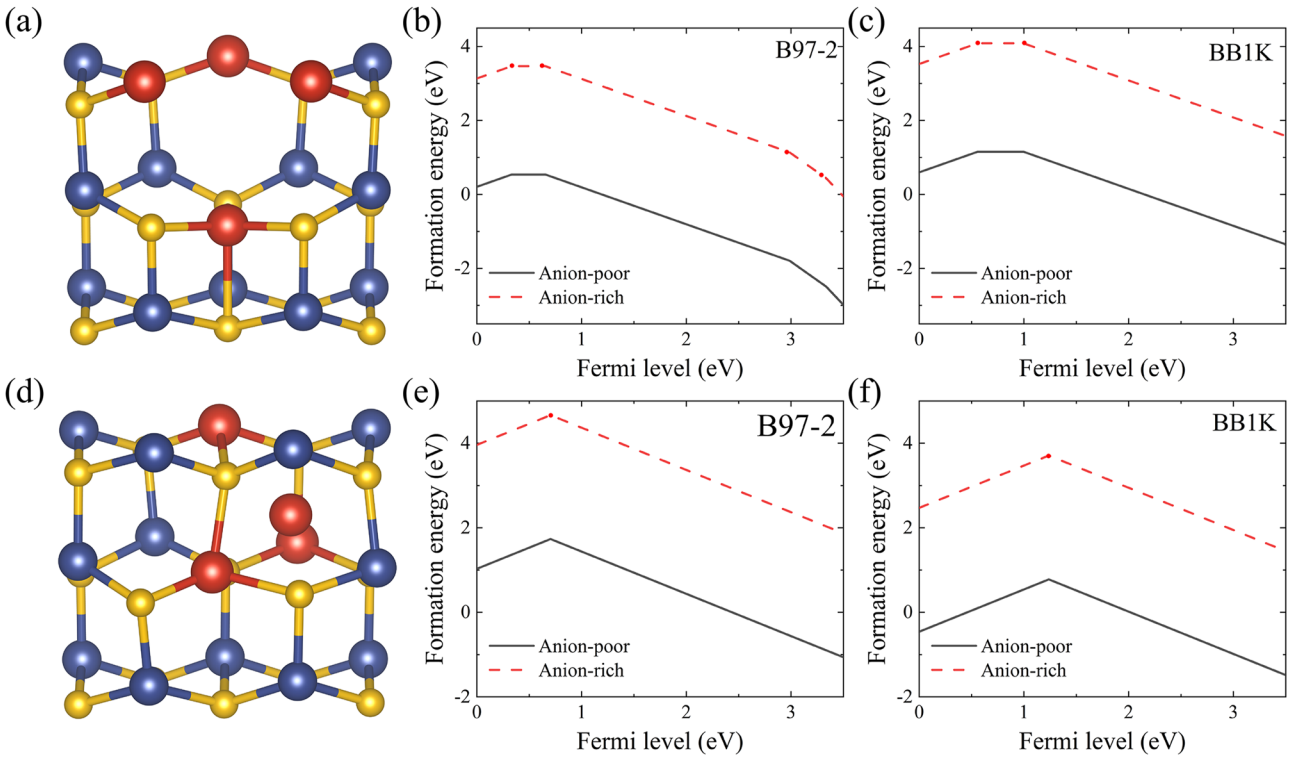

FIG. 2. Structures of (a) $4Mg_{Ga}$-V_N and (d) $3Mg_{Ga}$-Mg_i in −1 charge state. The blue, yellow, and red balls denote the Ga, N, and Mg atoms, respectively. Formation energies of (b) and (c) $4Mg_{Ga}$-V_N and (d) and (e) $3Mg_{Ga}$-Mg_i as a function of Fermi energy above the VBM calculated by B97-2 and BB1K functional, respectively. Anion-poor and anion-rich conditions are both given.

transition level at 0.704 (1.237) eV determined using B97-2 (BB1K). Both complexes neutralize a major compensating center in *p*-GaN and become acceptors that have smaller hole dissociation energies compared to the isolated Mg_{Ga} acceptor. Moreover, both complexes have lower formation energies in anion-poor conditions than isolated Mg_{Ga}, indicating that they can form at higher concentrations than isolated Mg_{Ga} in heavily doped GaN:Mg. We have calculated the equilibrium defect concentrations using the code SC-FERMI,[52] as shown in Fig. 3.

Our calculations have, therefore, shown that the major compensating donor centers V_N and Mg_i in *p*-GaN:Mg can be neutralized by binding to multiple Mg_{Ga} acceptors. Through forming a cluster with Mg_3N_2 stoichiometry and an additional Mg_{Ga}, a large Mg-rich acceptor complex forms that is a better acceptor than isolated Mg_{Ga}, with lower hole localization energies and lower formation energies in anion-poor conditions. Following this pattern, we can expect that even larger Mg-rich complexes can form in *p*-GaN and contribute to the *p*-type conductivity. Mg-rich pyramidal defects in *p*-GaN have been observed previously in experimental studies. For example, in MOVPE Mg-doped GaN, Vennéguès *et al.*[53] found that these pyramidal defects are Mg rich and present in all studied films, independent of the doping level. Recently, maps of the electrostatic potential provided by off-axis electron holography have confirmed that the highest carrier concentration was achieved in the regions with the highest dopant concentration of 2×10^{20} cm^{-3}, despite the presence of a high density of Mg-rich clusters revealed by correlating atom probe tomography.[54] We propose that larger complex acceptors can have lower hole localization energies and, with the right size, form at least some of the shallow acceptors observed in conductive *p*-GaN. Kozodoy *et al.*[55] investigated heavily Mg-doped GaN through variable-temperature Hall-effect measurements and found that the effective acceptor energy depth decreases from 190 to 112 meV and the compensation ratio increases as the dopant density is increased to the high values typically used in device applications. However, there is likely to be an optimum size of the Mg-rich complex since, in *p*-GaN, V_N has a charge state of +3, and its formation energy will reduce drastically as the Fermi level moves closer to the VBM. As for Mg_i, its formation energy is not as low as V_N in *p*-GaN (though it will still decrease by twice the decrease in Fermi level as it shifts toward the VBM). However, heavy Mg-doping will increase the concentration of Mg_i.[25] Liliental-Weber *et al.*[56] determined at atomic resolution of the Mg-rich hexagonal pyramids and truncated pyramids in GaN:Mg, to which they attributed the commonly observed decrease in acceptor concentration in the heavily doped material.

The BL band is probably due to a Mg-rich cluster that contains a V_N since it is observed only in heavily doped GaN:Mg samples grown by HVPE or MOCVD,[1] and Hautakangas *et al.*[17] suggested

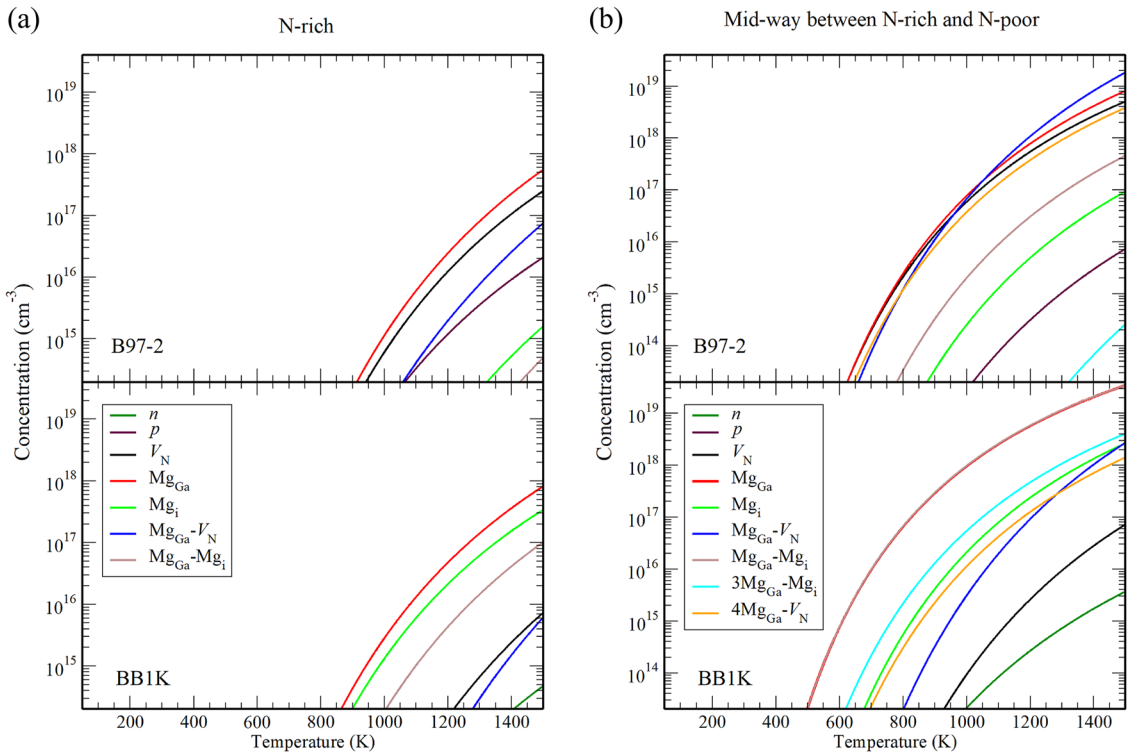

FIG. 3. The calculated equilibrium concentrations of electrons (*n*), holes (*p*), and defects (complexes) studied in this work as a function of temperature. Results from both exchange and correlation density functionals are shown for (a) N-rich condition and (b) mid-way between the N-rich and N-poor conditions.

that neutral or negative complexes involving isolated V_N exist in semi-insulating and *p*-type MOCVD-grown GaN. In contrast, the BL band is not observed in *p*-type, Mg-doped GaN grown by MBE, and Hautakangas *et al.*[17] observed no vacancies in MBE-grown GaN:Mg samples. This trend is consistent with that observed for the *p*-type conductivity; it is reported that the maximum hole concentration can be one order of magnitude higher in MBE-grown[57] GaN:Mg than MOCVD-grown samples. As V_N has a higher concentration in MOCVD-grown samples than in MBE-grown ones, we expect that the dominant compensating isolated donors in MOCVD samples will be V_N and Mg_i, and mostly Mg_i in MBE-grown samples. Therefore, the overall compensating effect is more prominent in MOCVD samples, resulting in a different doping efficiency. The activation of *p*-type conductivity by annealing in MOCVD samples is probably due to the dissociation of large open volume defects into N monovacancy complexes, as can be seen in the PAS measurements of Ref. 17.

Several studies have proposed that the desired Mg_{Ga} acceptor in as-grown MOCVD GaN:Mg is passivated by H donor-type defects by forming complexes of Mg_{Ga}-H_i and that postgrowth annealing can dissociate those complexes and activate the isolated Mg_{Ga} as acceptors.[58] We argue that H, as a donor-type impurity, can passivate any form of acceptor in the sample,[22] including the large complexes we propose here, so that H passivation is probably an additional process rather than a limiting factor in Mg doping.

IV. CONCLUSIONS

In conclusion, we show that to achieve *p*-type conductivity in GaN:Mg, the major compensating centers V_N and Mg_i can be passivated by binding to Mg_{Ga} centers. Such complexing can reduce the number of holes localized on isolated Mg_{Ga} and form large Mg-rich acceptor complexes that have smaller hole localization energies and lower formation energies than isolated Mg_{Ga}. There are two kinds of such large complexes, which differ as to whether they contain a V_N. By comparison with experimental observations of the optical and electronic properties of GaN:Mg, we find that the complexes that contain a V_N are likely to prevail in MOCVD-grown GaN but not in MBE-grown GaN, where only those containing Mg_i and Mg_{Ga} should be observed. Similarly, the BL band observed in MOCVD- and not MBE-grown GaN is attributed to V_N-containing complexes. The requirement for annealing after growth in MOCVD- but not MBE-grown GaN to activate *p*-type conductivity is attributed to the need to dissociate large open volume defects from N monovacancy complexes. Future work will investigate the influence of complexes that contain more than one V_N on *p*-type conductivity.

ACKNOWLEDGMENTS

We are grateful to Professor Anthony Cheetham for many fruitful and enjoyable discussions relating to materials chemistry

and physics. This paper continues our previous exciting collaboration with Aron Walsh, to whom we are indebted. The EPSRC is acknowledged for funding (Grant Nos. EP/K038419, EP/I03014X, and EP/K016288). Computational resources were provided by the ARCHER service through the Materials Chemistry High End Computing Consortium funded by EPSRC Grant No. EP/L000202, EP/R029431 and EP/X035859. GuangDong Basic and Applied Basic Research Foundation (Grant No. 2022A1515111156) is acknowledged.

AUTHOR DECLARATIONS

Conflict of Interest

The authors have no conflicts to disclose.

Author Contributions

Zijuan Xie: Conceptualization (equal); Investigation (lead); Validation (equal); Visualization (equal); Writing – original draft (equal); Writing – review & editing (equal). **John Buckeridge**: Conceptualization (equal); Formal analysis (equal); Investigation (equal); Methodology (equal); Software (lead); Writing – review & editing (equal). **C. Richard A. Catlow**: Conceptualization (equal); Funding acquisition (equal); Methodology (equal); Supervision (lead); Writing – review & editing (equal). **Anping Zhang**: Data curation (equal); Formal analysis (equal); Validation (equal). **Thomas W. Keal**: Methodology (equal); Software (lead). **Paul Sherwood**: Software (equal). **You Lu**: Formal analysis (equal); Methodology (equal); Software (equal). **Scott M. Woodley**: Funding acquisition (equal); Methodology (equal); Resources (lead). **Alexey A. Sokol**: Conceptualization (equal); Methodology (equal).

DATA AVAILABILITY

The data that support the findings of this study are available from the corresponding authors upon reasonable request.

REFERENCES

[1] M. A. Reshchikov, P. Ghimire, and D. O. Demchenko, Phys. Rev. B **97**, 205204 (2018).
[2] U. Kaufmann, P. Schlotter, H. Obloh, K. Köhler, and M. Maier, Phys. Rev. B **62**, 10867 (2000).
[3] U. Kaufmann, M. Kunzer, M. Maier, H. Obloh, A. Ramakrishnan, B. Santic, and P. Schlotter, Appl. Phys. Lett. **72**, 1326 (1998).
[4] S. Lany and A. Zunger, Appl. Phys. Lett. **96**, 142114 (2010).
[5] J. L. Lyons, A. Janotti, and C. G. Van De Walle, Phys. Rev. Lett. **108**, 156403 (2012).
[6] Y. Y. Sun, T. A. Abtew, P. Zhang, and S. B. Zhang, Phys. Rev. B **90**, 165301 (2014).
[7] D. O. Demchenko, I. C. Diallo, and M. A. Reshchikov, Phys. Rev. B **97**, 205205 (2018).
[8] J. Buckeridge, C. R. A. Catlow, D. O. Scanlon, T. W. Keal, P. Sherwood, M. Miskufova, A. Walsh, S. M. Woodley, and A. A. Sokol, Phys. Rev. Lett. **114**, 016405 (2015).
[9] B. Monemar, P. P. Paskov, G. Pozina, C. Hemmingsson, J. P. Bergman, T. Kawashima, H. Amano, I. Akasaki, T. Paskova, S. Figge, D. Hommel, and A. Usui, Phys. Rev. Lett. **102**, 235501 (2009).
[10] B. Monemar, P. P. Paskov, G. Pozina, C. Hemmingsson, J. P. Bergman, S. Khromov, V. N. Izyumskaya, V. Avrutin, X. Li, H. Morkoç, H. Amano, M. Iwaya, and I. Akasaki, J. Appl. Phys. **115**, 053507 (2014).
[11] G. Callsen, M. R. Wagner, T. Kure, J. S. Reparaz, M. Bügler, J. Brunnmeier, C. Nenstiel, A. Hoffmann, M. Hoffmann, J. Tweedie, Z. Bryan, S. Aygun, R. Kirste, R. Collazo, and Z. Sitar, Phys. Rev. B **86**, 075207 (2012).
[12] A. K. Singh, K. P. O'Donnell, P. R. Edwards, K. Lorenz, M. J. Kappers, and M. Bońkowski, Sci. Rep. **7**, 41982 (2017).
[13] E. R. Glaser, M. Murthy, J. A. Freitas, D. F. Storm, L. Zhou, and D. J. Smith, Phys. B **401–402**, 327 (2007).
[14] J. J. Davies, Phys. Rev. B **87**, 235208 (2013).
[15] M. E. Zvanut, J. Dashdorj, U. R. Sunay, J. H. Leach, and K. Udwary, J. Appl. Phys. **120**, 135702 (2016).
[16] S. B. Zhang, S. H. Wei, and A. Zunger, Phys. Rev. Lett. **84**, 1232 (2000).
[17] S. Hautakangas, J. Oila, M. Alatalo, K. Saarinen, L. Liszkay, D. Seghier, and H. P. Gislason, Phys. Rev. Lett. **90**, 137402 (2003).
[18] T. Obata, N. Matsumura, K. Ogiwara, H. Hirayama, Y. Aoyagi, and K. Ishibashi, Phys. Status Solidi **3**, 1775 (2006).
[19] S. M. Myers, A. F. Wright, M. Sanati, and S. K. Estreicher, J. Appl. Phys. **99**, 113506 (2006).
[20] Q. Yan, A. Janotti, M. Scheffler, and C. G. Van De Walle, Appl. Phys. Lett. **100**, 142110 (2012).
[21] D. Lee, B. Mitchell, Y. Fujiwara, and V. Dierolf, Phys. Rev. Lett. **112**, 205501 (2014).
[22] F. A. Reboredo and S. T. Pantelides, Phys. Rev. Lett. **82**, 1887 (1999).
[23] M. A. Reshchikov, D. O. Demchenko, J. D. McNamara, S. Fernández-Garrido, and R. Calarco, Phys. Rev. B **90**, 035207 (2014).
[24] G. Miceli and A. Pasquarello, Phys. Rev. B **93**, 165207 (2016).
[25] U. Wahl, L. M. Amorim, V. Augustyns, A. Costa, E. David-Bosne, T. A. L. Lima, G. Lippertz, J. G. Correia, M. R. Da Silva, M. J. Kappers, K. Temst, A. Vantomme, and L. M. C. Pereira, Phys. Rev. Lett. **118**, 095501 (2017).
[26] U. Wahl, J. G. Correia, Â.R. G. Costa, E. David-Bosne, M. J. Kappers, M. R. da Silva, G. Lippertz, T. A. L. Lima, R. Villarreal, A. Vantomme, and L. M. C. Pereira, Adv. Electron. Mater. **7**, 2100345 (2021).
[27] U. Wahl, J. G. Correia, A. R. G. Costa, T. A. L. Lima, J. Moens, M. J. Kappers, M. R. Da Silva, L. M. C. Pereira, and A. Vantomme, Phys. Rev. B **105**, 184112 (2022).
[28] A. A. Sokol, S. T. Bromley, S. A. French, C. R. A. Catlow, and P. Sherwood, Int. J. Quantum Chem. **99**, 695 (2004).
[29] P. Sherwood, A. H. de Vries, M. F. Guest, G. Schrecken-bach, C. A. Catlow, S. A. French, A. A. Sokol, S. T. Bromley, W. Thiel, A. J. Turner, S. Billeter, F. Terstegen, S. Thiel, J. Kendrick, S. C. Rogers, J. Casci, M. Watson, F. King, E. Karlsen, M. Sjøvoll, A. Fahmi, A. Schäfer, and C. Lennartz, J. Mol. Struct.: THEOCHEM **632**, 1 (2003).
[30] M. Miskufova, Ph.D thesis, University College London, 2011.
[31] S. Metz, J. Kästner, A. A. Sokol, T. W. Keal, and P. Sherwood, Wiley Interdiscip. Rev.: Comput. Mol. Sci. **4**, 101 (2014).
[32] M. F. Guest, I. J. Bush, H. J. Van Dam, P. Sherwood, J. M. H. Thomas, J. H. Van Lenthe, R. W. Havenith, and J. Kendrick, Mol. Phys. **103**, 719 (2005).
[33] J. D. Gale, J. Chem. Soc., Faraday Trans. **93**, 629 (1997).
[34] P. J. Wilson, T. J. Bradley, and D. J. Tozer, J. Chem. Phys. **115**, 9233 (2001).
[35] C. Adamo and V. Barone, J. Chem. Phys. **110**, 6158 (1999).
[36] J. Heyd, G. E. Scuseria, and M. Ernzerhof, J. Chem. Phys. **124**, 219906 (2006).
[37] W. Stevens, M. Krauss, H. Basch, and P. Jasien, Can. J. Chem. **70**, 612 (1992).
[38] F. Weigend and R. Ahlrichs, Phys. Chem. Chem. Phys. **7**, 3297 (2005).
[39] Y. Zhao, B. J. Lynch, and D. G. Truhlar, J. Phys. Chem. A **108**, 2715 (2004).
[40] Z. Xie, Y. Sui, J. Buckeridge, C. R. A. Catlow, T. W. Keal, P. Sherwood, A. Walsh, M. R. Farrow, D. O. Scanlon, S. M. Woodley, and A. A. Sokol, J. Phys. D. Appl. Phys. **52**, 335104 (2019).
[41] A. Walsh, J. Buckeridge, C. R. A. Catlow, A. J. Jackson, T. W. Keal, M. Miskufova, P. Sherwood, S. A. Shevlin, M. B. Watkins, S. M. Woodley, and A. A. Sokol, Chem. Mater. **25**, 2924 (2013).
[42] D. J. Wilson, A. A. Sokol, S. A. French, and C. R. A. Catlow, "The Rôle of defects in photographic latent image formation," in *Materials Research Society Symposium Proceedings* (MRS, 2005), Vol. 848.
[43] A. A. Sokol, S. A. French, S. T. Bromley, C. R. A. Catlow, H. J. J. van Dam, and P. Sherwood, Faraday Discuss. **134**, 267 (2007).

[44]C. R. A. Catlow, A. A. Sokol, and A. Walsh, Chem. Commun. **47**, 3386 (2011).
[45]Z. Xie, Y. Sui, J. Buckeridge, A. A. Sokol, T. W. Keal, and A. Walsh, Appl. Phys. Lett. **112**, 262104 (2018).
[46]Z. Xie, Y. Sui, J. Buckeridge, C. R. A. Catlow, T. W. Keal, P. Sherwood, A. Walsh, D. O. Scanlon, S. M. Woodley, and A. A. Sokol, Phys. Status Solidi A **214**, 1600445 (2017).
[47]D. O. Demchenko and M. A. Reshchikov, Phys. Rev. Lett. **115**, 029701 (2015).
[48]J. Buckeridge, C. R. A. Catlow, D. O. Scanlon, T. W. Keal, P. Sherwood, M. Miskufova, A. Walsh, S. M. Woodley, and A. A. Sokol, Phys. Rev. Lett. **115**, 029702 (2015).
[49]D. O. Demchenko and M. A. Reshchikov, Appl. Phys. Lett. **118**, 142103 (2021).
[50]S. Limpijumnong and C. G. Van de Walle, Phys. Rev. B **69**, 035207 (2004).
[51]F. Tuomisto, Proc. SPIE **8625**, 86250G (2013).
[52]J. Buckeridge, Comput. Phys. Commun. **244**, 329 (2019).
[53]P. Vennéguès, M. Benaissa, B. Beaumont, E. Feltin, P. De Mierry, S. Dalmasso, M. Leroux, and P. Gibart, Appl. Phys. Lett. **77**, 880 (2000).
[54]L. Amichi, I. Mouton, E. Di Russo, V. Boureau, F. Barbier, A. Dussaigne, A. Grenier, P. H. Jouneau, C. Bougerol, and D. Cooper, J. Appl. Phys. **127**, 065702 (2020).
[55]P. Kozodoy, H. Xing, S. P. DenBaars, U. K. Mishra, A. Saxler, R. Perrin, S. Elhamri, and W. C. Mitchel, J. Appl. Phys. **87**, 1832 (2000).
[56]Z. Liliental-Weber, T. Tomaszewicz, D. Zakharov, J. Jasinski, and M. A. O'Keefe, Phys. Rev. Lett. **93**, 206102 (2004).
[57]I. P. Smorchkova, E. Haus, B. Heying, P. Kozodoy, P. Fini, J. P. Ibbetson, S. Keller, S. P. DenBaars, J. S. Speck, and U. K. Mishra, Appl. Phys. Lett. **76**, 718 (2000).
[58]S. Nakamura, N. Iwasa, M. S. Masayuki Senoh, and T. M. Takashi Mukai, Jpn. J. Appl. Phys. **31**, 1258 (1992).
[59]The formation energies of the configurations in the neutral and next-nearest neighbor cases; the corresponding +2/0 charge state are 2.55, 2.54 and 2.93 eV for the axial, basal-plane transition levels are 2.13, 2.05 and 2.22 eV above the VBM.